



PERGAMON



Atmospheric Environment 35 (2001) 6347–6360

ATMOSPHERIC  
ENVIRONMENT

www.elsevier.com/locate/atmosenv

# A climatology of $^7\text{Be}$ at four high-altitude stations at the Alps and the Northern Apennines

E. Gerasopoulos<sup>a,\*</sup>, P. Zanis<sup>b</sup>, A. Stohl<sup>c</sup>, C.S. Zerefos<sup>b</sup>, C. Papastefanou<sup>a</sup>,  
W. Ringer<sup>d</sup>, L. Tobler<sup>e</sup>, S. Hübener<sup>f</sup>, H.W. Gäggeler<sup>e,f</sup>, H.J. Kanter<sup>g</sup>,  
L. Tositti<sup>h</sup>, S. Sandrini<sup>h</sup>

<sup>a</sup> Nuclear Physics Department, Aristotle University of Thessaloniki, 54006 Thessaloniki, Greece

<sup>b</sup> Laboratory of Atmospheric Physics, Aristotle University of Thessaloniki, Greece

<sup>c</sup> Lehrstuhl für Bioklimatologie und Immissionsforschung, University of Munich, Freising, Germany

<sup>d</sup> Federal Office of Agrobiolology, Linz, Austria

<sup>e</sup> Paul Scherrer Institute, Villigen PSI, Switzerland

<sup>f</sup> Departement für Chemie und Biochemie, University of Bern, Switzerland

<sup>g</sup> Fraunhofer Institute, Garmisch-Partenkirchen, Germany

<sup>h</sup> Environmental Radiochemistry Laboratory, University of Bologna, Italy

Received 4 May 2000; received in revised form 20 July 2001; accepted 26 July 2001

## Abstract

The  $^7\text{Be}$  activity concentrations measured from 1996 to 1998 at four high-altitude stations, Jungfraujoch—Switzerland, Zugspitze—Germany, Sonnblick—Austria and Mt. Cimone—Italy, were analyzed in combination with a set of meteorological and atmospheric parameters such as the tropopause height, relative and specific humidity and also in conjunction with 3D back-trajectories in order to investigate the climatological features of  $^7\text{Be}$ . A frequency distribution analysis on  $^7\text{Be}$  activity concentrations revealed the existence of two concentration classes around 1.5 and 6 mBq m<sup>-3</sup> and a transition class between the two modes of the distribution at 3–4 mBq m<sup>-3</sup>. Cross-correlation analysis performed between  $^7\text{Be}$  and a number of meteorological and atmospheric parameters at the first three stations showed a strong negative correlation with relative humidity (–0.56, –0.51, –0.41) indicating the importance of wet scavenging as a controlling mechanism. Also, the positive correlation with the height of 3-days back-trajectories and tropopause height (+0.49/+0.43, +0.59/+0.36, +0.44/+0.38) shows that downward transport from the upper or middle to lower troposphere within anticyclonic conditions plays also an important role. Trajectory statistics showed that low  $^7\text{Be}$  concentrations typically originate from lower-altitude subtropical ocean areas, while high concentrations arrive from the north and high altitudes, as is characteristic for stratospheric intrusions. Although the  $^7\text{Be}$  activity concentrations are highly episodic, the monthly means indicate an annual cycle with a late-summer maximum at all stations. The correlation coefficients calculated for monthly means of the  $^7\text{Be}$  and atmospheric data suggest that the main predictor controlling the seasonality of the  $^7\text{Be}$  concentrations is tropopause height (+0.76, +0.56, +0.60), reflecting more vertical transport from upper tropospheric levels into the lower troposphere during the warm season than during the cold season. © 2001 Elsevier Science Ltd. All rights reserved.

**Keywords:**  $^7\text{Be}$ ; Alps; Climatology; Stratospheric intrusions; Surface ozone

\*Corresponding author. Tel.: +30-31-998202; fax: +30-31-998058.

E-mail address: egera@skiathos.physics.auth.gr (E. Gerasopoulos).

## 1. Introduction

The bombardment of atmospheric constituents by cosmic rays (CR) leads to the production of a host of

isotopes, within a range of half-lives from some minutes up to millions of years. One of them is  $^7\text{Be}$ , a cosmogenic gamma emitting (477.6 keV) radionuclide with radioactive decay half-life of 53.3 days. It is formed through spallation reactions leading to the fragmentation of light atmospheric nuclei, primarily  $^{12}\text{C}$ ,  $^{14}\text{N}$  and  $^{16}\text{O}$  (Lal and Peters, 1967; Masarik and Beer, 1999).

Lal and Peters (1967) have shown that production rates are decreasing with atmospheric depth. This fact, in combination with the increase of the atmospheric density and therefore the availability of target nuclei for spallation reactions, leads to the existence of a maximum in the production rate at about 20 km. The relatively high production rates of  $^7\text{Be}$  in the upper troposphere, combined with transport from the lower stratosphere to the upper troposphere, normally maintain a steep vertical concentration gradient between the upper and the lower troposphere (Feely et al., 1989). The source functions of radioactive isotopes depending mainly on latitude and altitude have been determined in detail by Benioff (1956), Lal et al. (1958), Lal and Peters (1962), O'Brien (1979) and others, concluding that only 33% of the  $^7\text{Be}$  production takes place in the troposphere and particularly in the upper troposphere, while the rest is produced in the stratosphere.

Soon after  $^7\text{Be}$  atoms are formed, they become attached to ambient aerosol particles in the accumulation mode (0.4–2  $\mu\text{m}$ ) (Papastefanou and Ioannidou, 1995). Since the process of attachment is irreversible the fate of the  $^7\text{Be}$  atoms is henceforth determined by the mechanisms governing the removal and transport of the aerosols. The tropospheric residence time of these aerosols can vary from a few days to a few weeks, depending on meteorological conditions. The mean residence time in the troposphere is of the order of about 10 days (Jaenicke, 1988) to 30 days (Gavini et al., 1974; Koch et al., 1996).

The average  $^7\text{Be}$  concentration in the lower stratosphere between  $11^\circ$  and  $60^\circ\text{N}$  observed by Dutkiewicz and Husain (1985) was  $165\text{ mBq m}^{-3}$ , while in the upper troposphere the concentrations were generally  $<40\text{ mBq m}^{-3}$ . On average, the tropospheric production rate and the concentration of  $^7\text{Be}$  are  $810\text{ atoms m}^{-2}\text{ s}^{-1}$  and  $12.5\text{ mBq m}^{-3}$ , respectively (UNSCEAR, 2000). On the other hand, concentrations at surface levels fluctuate normally around  $3.5\text{ mBq m}^{-3}$  (Reiter et al., 1983; Dutkiewicz and Husain, 1985; Brost et al., 1991; Gägger, 1995). Thus, air coming from the upper troposphere and especially the stratosphere can be identified by its enhanced  $^7\text{Be}$  levels.

$^7\text{Be}$  concentrations follow certain time variations, the most common of which are the 11-years cycle of solar activity and the annual cycle (Koch and Mann, 1996). The vast majority of the studies conclude that  $^7\text{Be}$  surface concentrations at northern mid-latitudes show a maximum in late summer (Reiter et al., 1983; Feely et al.,

1989). According to Feely et al. (1989) there are four factors controlling the  $^7\text{Be}$  seasonal variation: (a) wet scavenging, (b) stratosphere-to-troposphere exchange, (c) downward transfer in the troposphere, and (d) transport between lower and higher latitudes.

Since most of the  $^7\text{Be}$  resides in the stratosphere, it has been used in many studies as a tracer of stratosphere-to-troposphere exchange (STE) (Danielsen, 1968; Husain et al., 1977; Elbern et al., 1997; Scheel et al., 1999; Zanis et al., 1999; Stohl et al., 2000). Cross-tropopause flux estimation is still a topic of great scientific interest due to the aircraft emissions at the tropopause level and also because there are large discrepancies between different studies regarding the relative importance of STE and photochemistry for tropospheric ozone (Roelofs and Lelieveld, 1997).

The current study presents an analysis of three years of  $^7\text{Be}$  data from four alpine stations: Jungfraujoch—Switzerland, Zugspitze—Germany, Sonnblick—Austria, and Mt. Cimone—Italy. The aim is to depict the main climatological characteristics of  $^7\text{Be}$  and reveal the mechanisms that they are subject to. For this purpose a set of supplementary meteorological and atmospheric data was used.

## 2. Data and methods

Over the past years  $^7\text{Be}$  measurements have been conducted at four elevated alpine stations, Jungfraujoch (JFJ), Switzerland ( $07^\circ59'\text{E}/46^\circ32'\text{N}$ , 3580 m asl), Zugspitze (ZUG), Germany ( $10^\circ59'\text{E}/47^\circ25'\text{N}$ , 2962 m asl), Sonnblick (SBK), Austria ( $12^\circ58'\text{E}/47^\circ03'\text{N}$ , 3106 m asl) and Mt. Cimone (MTC), Italy ( $10^\circ42'\text{E}/44^\circ12'\text{N}$ , 2165 m asl). The former three of them are located along the mountain chain of the Alps while the fourth one is situated in the Northern Apennines as shown in Fig. 1.

On a routine basis, all four stations use the same type of air-samplers equipped with flowmeters for flux stabilization during sampling and volume integration at the end of each sampling. Air flowrates vary from 32 to  $68\text{ m}^3\text{ h}^{-1}$ . The air-filters used are made of either glass fiber or cellulose nitrate. After sampling they are folded and pressed into a plastic container. Finally, high-resolution gamma spectrometry is applied for the acquisition of the spectrum, using coaxial or well-type detectors. At all stations the total uncertainty due to both sampling procedures and counting statistics is of the order of 10% and the calculated activities are routinely corrected to standard temperature–pressure (STP) conditions. The quality of the  $^7\text{Be}$  data and the comparability between the stations discussed in this paper has been proved by adequate testing during an intercomparison exercise (Tositti et al., 2001).

At JFJ, the  $^7\text{Be}$  measurements are carried out regularly with a time resolution of 48 h since 4 April

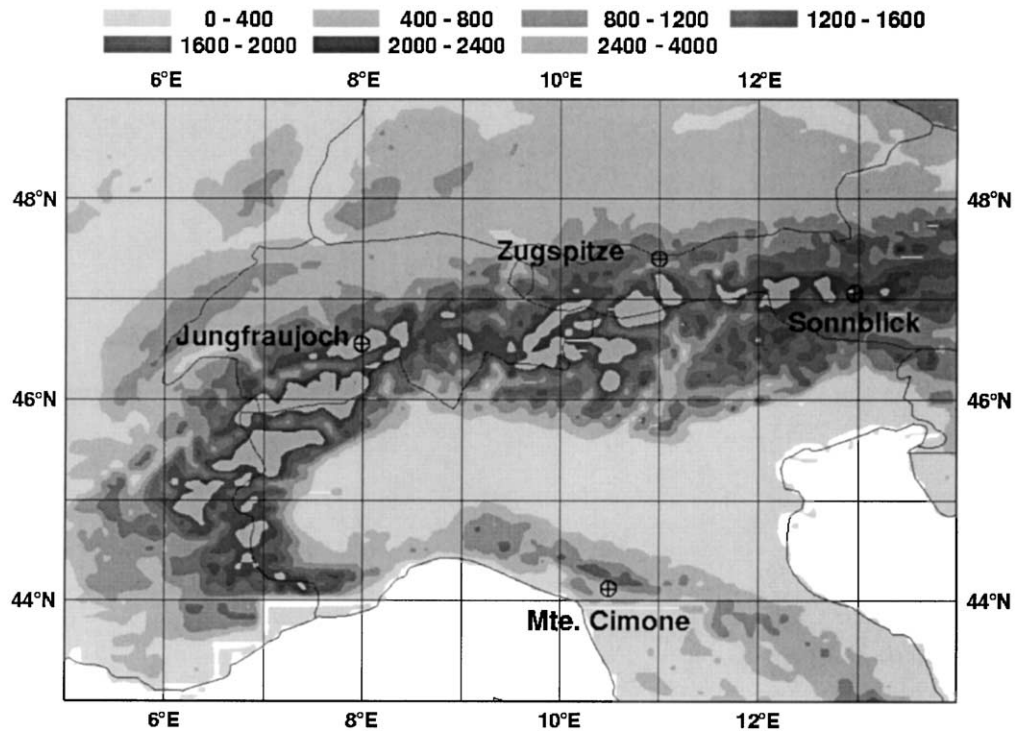


Fig. 1. Alpine region topography (m asl) and location of the measurement stations.

1996. The  $^7\text{Be}$  data used in this study cover the period from 4 April 1996 to 1 August 1999.  $^7\text{Be}$  measurements are also performed regularly at both ZUG and SBK with 24 h time resolution and the data sets used in this study cover the periods 5 January 1996–31 December 1998 and 20 June 1996–30 July 1999, respectively. Finally,  $^7\text{Be}$  measurements at MTC are available at irregular intervals from the period from 21 March 1996 to 31 December 1999.

For further analysis of the  $^7\text{Be}$  concentrations a supplementary data set of meteorological and other atmospheric parameters has been used, in order to identify the influence that each parameter has on the  $^7\text{Be}$  levels at alpine sites and to reveal the main controlling processes in a climatological aspect. The data sets for the three stations (JFJ, ZUG, SBK) cover the period from 1 January 1996 to 31 December 1998. MTC was not included in this analysis because  $^7\text{Be}$  sampling was not regular during these three years. The meteorological parameters included in the analysis were relative and specific humidity, while surface ozone concentrations were also compared with  $^7\text{Be}$ .

Apart from the meteorological parameters collected at the individual stations, a tropopause height timeseries was available for Payerne ( $6^{\circ}57'\text{E}/47^{\circ}48'\text{S}$ ), covering the period from 1 January 1996 to 31 December 1998. Tropopause height was available at both 00 and 12 h

UTC and daily means were extracted for use in the analysis. Finally, three-dimensional 10-day back trajectories ending at the position and altitudes above sea level of the mountain stations using the FLEXTRA trajectory model (Stohl et al., 1995; Stohl and Seibert, 1998), were calculated. FLEXTRA is driven with global analysis fields every 6 h and with 3-h forecast fields every other 3 h from the European Centre for Medium-Range Weather Forecasts (ECMWF, 1995) with a resolution of  $1^{\circ}$  longitude  $\times$   $1^{\circ}$  latitude. The model uses bicubic horizontal, quadratic vertical and linear time interpolation. The heights of an air mass (referred to as back-trajectory heights) 1, 2 and 3 days before its arrival at a station were used in the analysis.

To adjust with the different time resolution of  $^7\text{Be}$  measurements at JFJ, the related data sets were used to calculate bi-daily averages. Timeseries with a seasonal variation were deseasonalized and part of the analysis was repeated using the deseasonalized timeseries.

### 3. Results and discussion

#### 3.1. Frequency distribution of $^7\text{Be}$ concentrations

The four  $^7\text{Be}$  timeseries are presented graphically in Fig. 2. Basic statistics on  $^7\text{Be}$  concentrations at the four

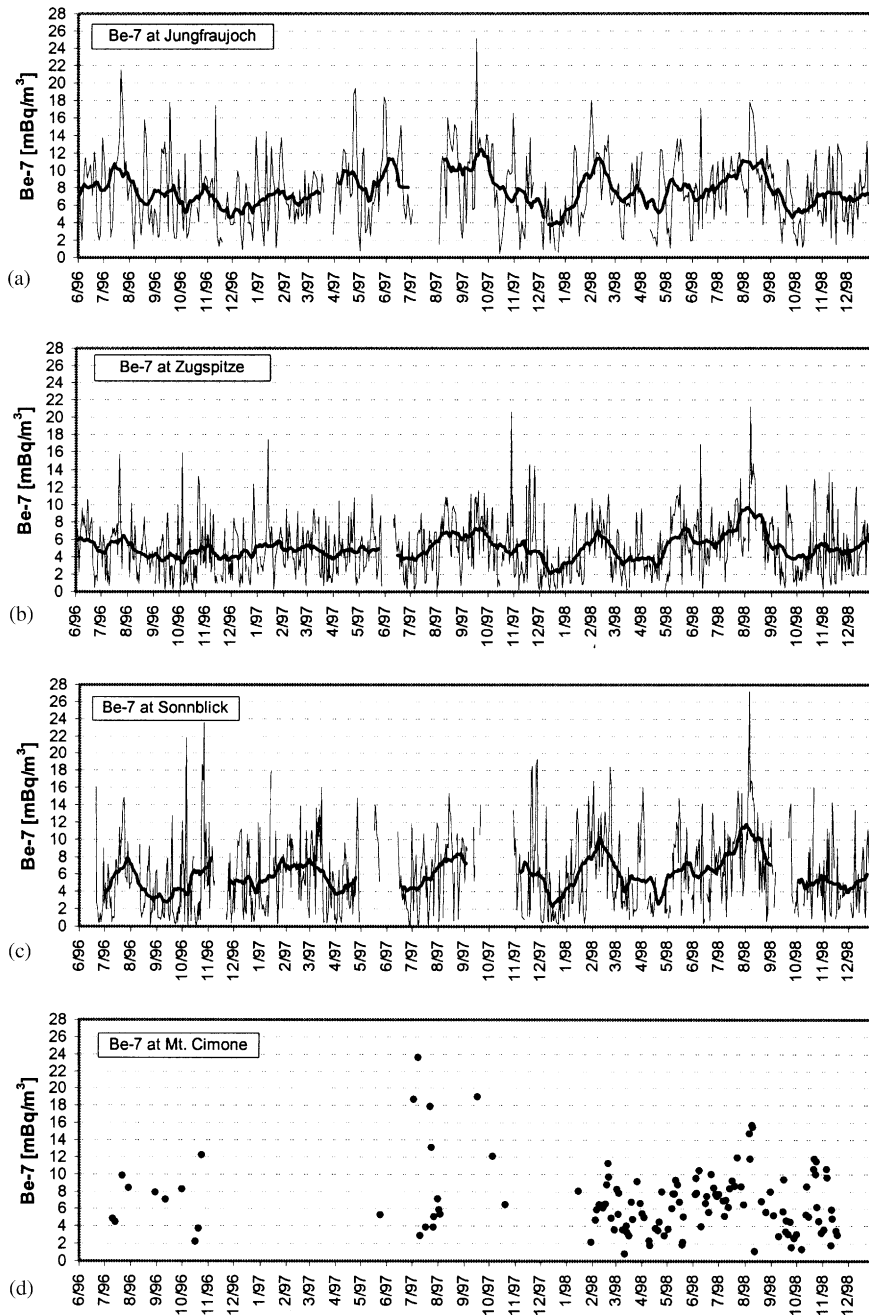


Fig. 2.  $^7\text{Be}$  timeseries at four alpine locations during the 1996–1998 period. The thick solid line represents a 30 days moving average fit.

alpine stations are shown in Table 1. Zanis et al. (1999), performing a frequency distribution analysis on a 9 months  $^7\text{Be}$  record at JFJ, suggested the possibility of interpreting the distribution as bi-modal, with each mode corresponding to a distinct class of meteorological conditions. In this study a frequency distribution analysis was carried out for each of the  $^7\text{Be}$  records.

The class intervals were set to  $1\text{ mBq m}^{-3}$  and all observations in a class interval were attributed to the interval mid-point. The resulting diagrams are presented in Fig. 3 where class frequencies are displayed by the black dots. It is seen that  $^7\text{Be}$  concentrations belong into two distinct classes, covering the lower and the higher values, respectively, and thus a sum of two Gaussian

Table 1  
Basic statistics of  $^7\text{Be}$  concentrations

$^7\text{Be}$ ( $\text{mBq m}^{-3}$ )						
Station ID	No. of obs.	Median	1st quartile	3rd quartile	Max	Min
JFJ	568	7.0	4.2	10.1	25.2	0.4
ZUG	1053	4.6	2.4	7.0	21.3	0.1
SBK	944	5.3	2.2	8.8	27.3	0.2
MTC	264	5.7	3.7	7.8	23.6	0.3

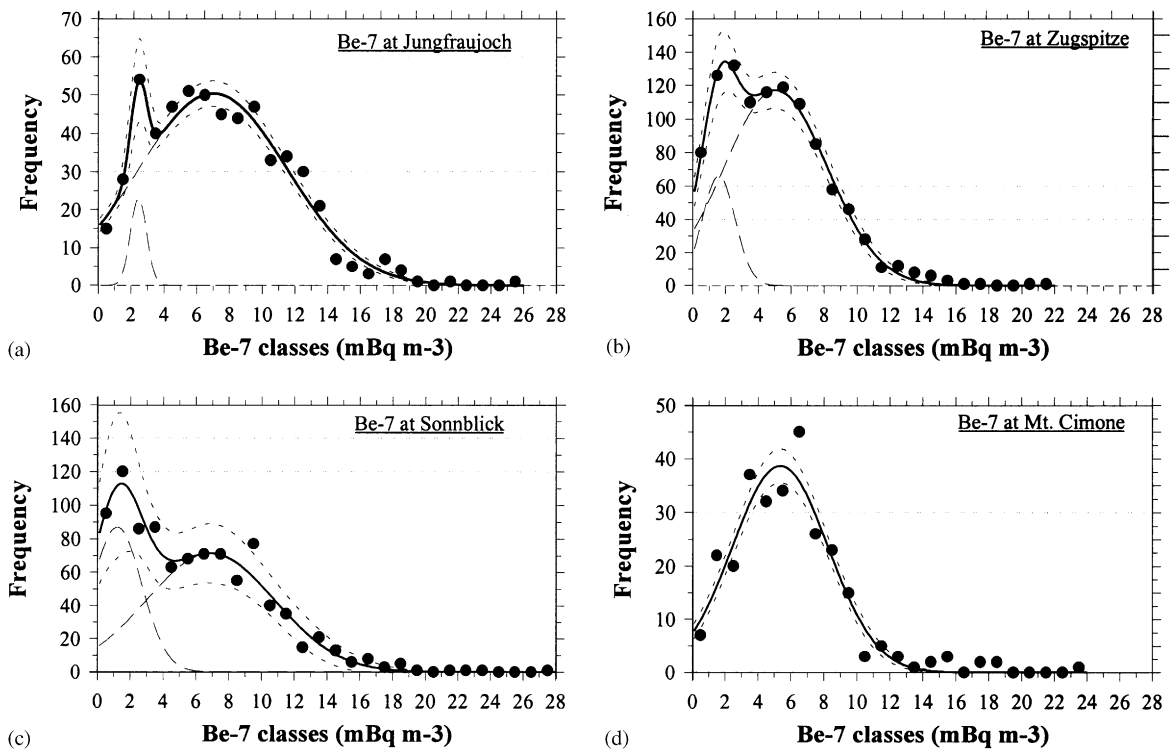


Fig. 3. Frequency distributions of  $^7\text{Be}$  concentrations for each site (dots). The dashed lines represent the normal distributions calculated through the fitting process, the thick solid line depicts the composite bi-modal distribution, whereas the dotted ones correspond to the standard error of the composite distribution.

functions was fitted on the resulting class frequencies. The mean and the standard deviation of both distributions were calculated. The fitted function explains 98% of the distributions variances with the exception of MTC for which a bi-modal distribution could not be statistically supported due to the lack of a sufficiently large amount of data. The results of the fitting procedure for each station are presented in Table 2.

The  $^7\text{Be}$  frequency distributions are bi-modal. The first mode is related to the lower values and has a mean of about  $1.5 \text{ mBq m}^{-3}$ . For JFJ the mean of this mode is somewhat higher and fewer values fall into this mode

because of the 48 h time resolution which smoothes away low values. The second mode represents the higher values, has a mean around  $6 \text{ mBq m}^{-3}$  and appears flatter than the first one. For ZUG the mean of the second class is lower due to the generally lower concentration levels at this station. A possible explanation for the observed deviation of the ZUG  $^7\text{Be}$  concentrations from the other stations is based on the special meteorological conditions that occur frequently at ZUG, namely increased cloud formation under northwesterly to northerly large-scale air flow, leading to increased rain out/wash out of aerosols. The data clearly show that

Table 2

Main characteristics (number of observations, mean value and standard deviation) of the two “normal” distributions that explain the  $^7\text{Be}$  concentrations frequency distribution<sup>a</sup>

Station ID	1st class			2nd class		
	No. of obs	Mean	Std	No. of obs	Mean	Std
JFJ	29 ± 10	2.5 ± 0.2	0.5 ± 0.1	574 ± 25	7.0 ± 0.2	4.5 ± 0.2
ZUG	167 ± 42	1.6 ± 0.1	1.0 ± 0.1	928 ± 63	5.1 ± 0.2	3.2 ± 0.2
SBK	331 ± 132	1.2 ± 0.2	1.5 ± 0.4	698 ± 127	6.9 ± 0.8	3.9 ± 0.7
MTC	—	—	—	284 ± 15	5.3 ± 0.2	2.9 ± 0.2

<sup>a</sup> Each value calculated by the fitting procedure is accompanied by its standard error.

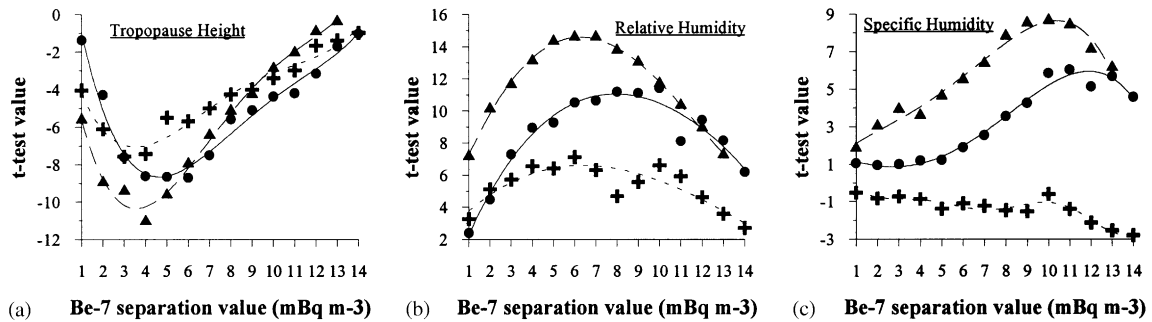


Fig. 4. *t*-Test values for the significance of the difference between the means of meteorological and other atmospheric parameters, when sorted according to a separation value of  $^7\text{Be}$ . All points indicate the *t*-test values and the lines constitute a polynomial function fitted on them. The presented data for JFJ (dots—solid line), ZUG (triangles—dashed dotted line), SBK (crosses—dotted line) are (a) tropopause height, (b) relative humidity, and (c) specific humidity.

peak  $^7\text{Be}$  concentrations caused by large-scale descending air are very similar to those measured at the other stations. The bimodality in the frequency distributions possible reflects the existence of different controlling mechanisms governing the two classes.

From the synthesis of the two Gaussian functions it can be concluded that there is a transition class between the two modes of the distributions at 3–4  $\text{mBq m}^{-3}$ . In order to show that different mechanisms are associated with the two modes, a supplementary analysis was performed, connecting  $^7\text{Be}$  concentration classes with a variety of meteorological and other atmospheric parameters.

For each  $^7\text{Be}$  record the meteorological and atmospheric data were successively sorted to two classes according to a hypothetical separation value of  $^7\text{Be}$ . The separation values of  $^7\text{Be}$  ranged from 1 to 14  $\text{mBq m}^{-3}$  and for each case two distinct classes of meteorological and atmospheric data were formed, connected with  $^7\text{Be}$  concentrations below and above the separation value, correspondingly. The statistical difference between the means of the two classes was checked using Student's *t*-test. The analysis was performed on both the original and the seasonally decomposed records, with the

exception of relative humidity for which a distinct seasonal cycle does not exist.

The results of the above analysis are presented in Fig. 4. For tropopause height (Fig. 4a), it is clearly evident that for all stations there is an outstanding pattern depicting a transition class of  $^7\text{Be}$  at 3–4  $\text{mBq m}^{-3}$ , for which the significance of the difference between the two means maximizes in absolute terms. The negative sign of the *t*-test values reflects the fact that the first tropopause height class has a smaller mean than the second class, which implies a positive correlation between  $^7\text{Be}$  and tropopause height. The difference between the means of the two tropopause height classes separated at the maximum *t*-test value lies in the range of 800–1000 m.

The picture is different for relative humidity (Fig. 4b). The obtained curves appear to be broader and the maximum *t*-test values are spread around the mean of each  $^7\text{Be}$  second class. This is mainly due to the fact that more than 50% of the relative humidity values are higher than 80% and thus lack the necessary variability in order to distinguish between the two  $^7\text{Be}$  classes. For the absolutely maximum *t*-test values the difference between the means of the two relative humidity classes is

Table 3

Cross-correlation coefficients between  $^7\text{Be}$  and relative humidity (RH) specific humidity (SH), surface ozone ( $\text{O}_3$ ), tropopause height (TRH) and back-trajectories height (BTRJH)<sup>a</sup>

	JFJ		ZUG		SBK	
	Raw	Residuals	Raw	Residuals	Raw	Residuals
TRH	(+) 0.43	(+) 0.37	(+) 0.36	(+) 0.35	(+) 0.38	(+) 0.35
BTRJH	(+) 0.49	—	(+) 0.59	—	(+) 0.44	—
RH	(-) 0.56	—	(-) 0.51	—	(-) 0.45	—
SH	(-) 0.03*	(-) 0.27	(-) 0.02*	(-) 0.25	(+) 0.07*	(-) 0.03*
$\text{O}_3$	(+) 0.35	(+) 0.40	(+) 0.42	(+) 0.51	(+) 0.34	(+) 0.44

<sup>a</sup>The column labeled as “Raw” corresponds to the correlation coefficients between raw data while the column labeled as “Residuals” corresponds to the correlation coefficients between the seasonal decomposed data. (+) and (–) indicate positive and negative correlation, respectively, whereas the values denoted by the asterisk are not significant at the 95% confidence level.

about 20%, in average. Finally, from specific humidity (Fig. 4c), the existence of a second maximum within the range 9–11  $\text{mBq m}^{-3}$  can be speculated, with the exception of SBK for which it is shown in section 3.3 (Table 3) that  $^7\text{Be}$  is not strongly correlated with specific humidity. The difference between the means of the two specific humidity classes lies in the range of 0.3–0.8  $\text{g kg}^{-1}$ .

From this result a second  $^7\text{Be}$  transition class could be possibly supported, which might imply the existence of a third distribution explaining the  $^7\text{Be}$  values above 10  $\text{mBq m}^{-3}$ . This is in accordance with Reiter et al. (1983) who showed that the total ogive of the  $^7\text{Be}$  frequency distribution was composed of three partial sections: (a) a linear normal distribution around 0.9  $\text{mBq m}^{-3}$  of the tropospheric values without stratospheric influx, (b) a linear normal distribution ranging from 2.6 to 7.4  $\text{mBq m}^{-3}$  of the values influenced by stratospheric intrusions, and (c) the range of values  $>7.4 \text{mBq m}^{-3}$  of the direct stratospheric intrusions near the station, without a long advection path. Apart from that, there have been many studies in which different thresholds of  $^7\text{Be}$  activity were used for identifying air masses of stratospheric origin. Reiter et al. (1984) used a 30% increase in  $^7\text{Be}$  values against the monthly mean as a criterion and Elbern et al. (1997) applied a definition of  $2\sigma$  increase against the running monthly mean, while others have selected a constant threshold of about 8  $\text{mBq m}^{-3}$  (Scheel et al., 1999; Sladkovic and Munzert, 1990; Stohl et al., 2000). Further discussion concerning the interpretation of the two  $^7\text{Be}$  transition classes is given in Section 3.3.

### 3.2. Correlation of $^7\text{Be}$ concentrations between the stations

The correlation of the  $^7\text{Be}$  concentrations between the alpine stations was investigated and discussed in this section. MTC was not included in this analysis because

of the sparseness of the data. For the correlation with JFJ two-day averages were calculated for ZUG and SBK. All correlation coefficients calculated are significant at the 99% significance level.

The correlation coefficients of  $^7\text{Be}$  concentration between JFJ-ZUG and JFJ-SBK are +0.53 and +0.42, correspondingly. This correlation is influenced by both the 48 h resolution of the  $^7\text{Be}$  concentrations at JFJ and the two-day averaging of the values at ZUG and SBK. The cross-correlation analysis between ZUG and SBK showed a maximum correlation coefficient of +0.70 for lag 1 day, with  $^7\text{Be}$  at ZUG coming first. This delay of 1 day at SBK is a result that could be expected taking into account the mostly westerly flow of the synoptic patterns in the middle latitudes and the fact that SBK is located 2° to the east from ZUG.

### 3.3. Correlation of $^7\text{Be}$ concentrations with atmospheric and meteorological parameters

The  $^7\text{Be}$  timeseries were analyzed in combination with a number of atmospheric and meteorological parameters, in order to clarify the role of each parameter for the  $^7\text{Be}$  concentration levels. Under this scope, the cross-correlation coefficients between  $^7\text{Be}$  and various parameters were calculated. The analysis was performed for both raw and deseasonalized data (where applicable) of relative humidity, specific humidity, surface ozone, tropopause height and back-trajectories height.

Table 3 shows the correlation coefficients corresponding to zero lag at which the maximum correlation, in terms of absolute values, was found. In the case of back-trajectories height the given correlation coefficient corresponds to the height of the air mass 3 days backwards along the trajectory, since it was better correlated with  $^7\text{Be}$  in comparison with heights 1 and 2 days backwards. Each of the values was tested for its significance level using two-tail significant points and analysis of variance (ANOVA).

Tropopause height at Payerne is positively correlated with  $^7\text{Be}$  concentrations at the three stations and therefore increased  $^7\text{Be}$  values are associated with high tropopause level, which is in turn associated with upper ridges (Vaughan and Price, 1991). Hence, the positive correlation between tropopause height and  $^7\text{Be}$  activity concentrations reflects both downward transport from the upper troposphere during anticyclonic conditions and less wet scavenging during these conditions. Although STE events are usually associated with upper-level troughs or cut-off lows, the stratospheric air typically descends stations within upper-level ridges (and surface anticyclones) following the troughs. Zanis et al. (1999) showed using composite maps of the geopotential height at 500 mbar that  $^7\text{Be}$  concentrations  $> 8 \text{ mBq m}^{-3}$  at JFJ were associated with an upper ridge over Switzerland. The strong correlation in combination with Fig. 4a, indicates that the day-to-day variability of the upper-troposphere synoptic situations is important for the transition between the two modes of the  $^7\text{Be}$  distribution. The even stronger positive correlation of  $^7\text{Be}$  with the 3-day back-trajectories height (+0.49, +0.59, and +0.54 for JFJ, ZUG, and SBK, respectively) reconfirms that high  $^7\text{Be}$  concentrations at the three alpine sites are related to transport of air masses originating from middle/upper troposphere levels to the lower tropospheric. It should be noted that there is no clear indication from the back-trajectories height for the direct influence of stratospheric air on the high  $^7\text{Be}$  concentrations at the three alpine sites. The use of more than 3 days back-trajectories increases the uncertainty of the air mass origin. Hence, the indirect influence from the stratosphere/troposphere exchange to lower tropospheric levels, depending on the upper-troposphere synoptic patterns and the time-scale of vertical mixing versus dilution, cannot be validated with certainty and thus should not be underestimated.

An important fraction of the  $^7\text{Be}$  variance is explained by relative humidity, emphasizing the role of wet scavenging. During high relative humidity conditions, condensation becomes more intense, resulting in increased wet scavenging rate of aerosols and thus of  $^7\text{Be}$  atoms attached to these aerosols. On the other hand, relative humidity has been used as a tracer to isolate events of stratosphere-to-troposphere exchange (STE), since stratospheric and tropospheric air masses are distinguished by very different water vapor concentrations (Bithell et al., 2000; Bonasoni et al., 2000). Thus, the anti-correlation between  $^7\text{Be}$  and relative humidity can be alternatively explained as events of downward transport of dry upper tropospheric or stratospheric air, but in this case one would expect specific humidity to be also a good predictor of  $^7\text{Be}$  concentrations, which is not the case as shown in Table 3. The calculated correlation coefficients for deseasonalized data, although statistically significant for JFJ and ZUG, do not explain such a

great fraction of the  $^7\text{Be}$  variance as relative humidity does, which leads to the conclusion that wet scavenging rather than downward transport is responsible for the statistically significant anti-correlation between the  $^7\text{Be}$  and the relative humidity. On the other hand, specific humidity has pointed out in Section 3.1 the possible existence of a second transition class of  $^7\text{Be}$  at about  $10 \text{ mBq m}^{-3}$  and as a result the possible existence of a third distribution, explaining  $^7\text{Be}$  concentrations with a direct effect from STE processes. One reason for this antiphase may be the relatively low number of  $^7\text{Be}$  values influenced by direct intrusion events within the three years data records. This fact, on the one hand, holds back the explicit emergence of a third distribution in Fig. 3 and obliterates part of the correlation, but, on the other hand, is able to introduce a transition class and perhaps preview the  $^7\text{Be}$  distribution pattern for more prolonged timeseries.

The mechanism that the correlation of relative humidity with  $^7\text{Be}$  expresses, was also investigated throughout the year by calculating correlation coefficients for each month. In general, the correlation coefficient between relative humidity and  $^7\text{Be}$  remains statistically invariable during the year, while the correlation coefficient between specific humidity and  $^7\text{Be}$  shows seasonality with high correlation (negative correlation,  $-0.50$  in average) during cold months (October to February). Thus, in the warm period wet scavenging dominates over transport for the determination of the better correlation between relative humidity and  $^7\text{Be}$  than between specific humidity and  $^7\text{Be}$ , while in the cold period transport becomes also important. However, taking into consideration, on the one hand, that the correlation of relative humidity with  $^7\text{Be}$  is always higher than the correlation between specific humidity and  $^7\text{Be}$  throughout the year and, on the other hand, that no practical discrimination between wet scavenging and transport is feasible, it can be concluded that wet scavenging remains a very important controlling mechanism throughout the year.

Surface ozone and deseasonalized surface ozone both show a significant and rather consistent positive correlation coefficient with  $^7\text{Be}$  concentrations for all stations (Table 3), indicating a significant covariance. Ozone taking its maximum values in the stratosphere can be used to identify air parcels of stratospheric origin. Especially, the existence of well-defined “bulges” of ozone-rich air below the tropopause level, as revealed from ozonesondes, has been widely connected with intrusion events (Austin and Follows, 1991; Kentarchos et al., 1998). However, surface ozone is difficult to interpret because the larger part of its variance can be attributed to photochemical processes associated with transport from pollution sources. Besides, there is great difficulty when interpreting high surface ozone concentrations, since there are different processes that may

coexist or conflict: (a) ozone-rich air parcels arriving from lower-stratosphere/upper-troposphere as a consequence of an intrusion event, (b) enhanced in situ photochemical production under anticyclonic conditions (Schuepbach et al., 1999). The fact that the anticyclonic conditions favor at the same time downward mixing of higher  $^7\text{Be}$ , intense photochemical ozone production and thermal convection of ozone precursors from the atmospheric boundary layer poses great difficulties to attribute their correlation to a common upper troposphere/lower stratosphere source.

### 3.4. Source regions of $^7\text{Be}$ and implications to horizontal transport

To study the source regions of  $^7\text{Be}$ , we combined the  $^7\text{Be}$  data with back trajectories. Back-trajectories were calculated every 3 h, so eight back-trajectories were available for each  $^7\text{Be}$  measurement. We used the method of Seibert et al. (1994) to attribute a measured value to all eight corresponding back-trajectories. Thus, the measured concentration is smeared out along the path the air has taken before arriving at the measurement location. After this is done for all trajectories, a so-called “concentration field” is obtained by averaging all values that occur within a grid box. We used a grid of  $1^\circ \times 1^\circ$  resolution and four vertical layers from the ground to 1500, 1500–3000, 3000–4500 and above 4500 m. This concentration field is subsequently smoothed and shows from where high or low concentrations are advected to the measurement sites. As the method needs many input data, we combined all measurement data from MTC, SBK and ZUG. Data from JFJ were not used, because of their coarser time resolution. The period used was 1995–1998, but note that SBK and MTC data were not available for 1995.

Fig. 5 shows that typically very low  $^7\text{Be}$  concentrations are advected from low levels, especially from ocean areas. The concentrations increase for the higher concentration field layers. For trajectories descending from above 4500 m, there is also a path of rather high  $^7\text{Be}$  concentrations (about  $8 \text{ mBq m}^{-3}$ ) seen that stretches from the northwest to the measurement sites. As stratospheric intrusions often reach the measurement sites via this pathway (see, e.g., Stohl et al., 2000), this likely reflects the influence of stratospheric intrusions on the  $^7\text{Be}$  concentrations at the mountain stations.

### 3.5. Case studies

The climatology of  $^7\text{Be}$  at the alpine sites implies the influence of different controlling mechanisms for the determination of the  $^7\text{Be}$  levels. In order to see the applicability of these processes in reality three case studies are presented. All three cases are during October

1996 and Fig. 6 shows the  $^7\text{Be}$ , relative humidity, specific humidity and surface  $\text{O}_3$  daily values at Zugspitze during this month. The tropopause height over Payerne is also shown.

*Case I (2 October 1996)—low  $^7\text{Be}$  concentration:* Fig. 6 shows a decrease of  $^7\text{Be}$  concentration on 2 October down to about  $0.2 \text{ mBq m}^{-3}$ . At the same time RH increases from about 60% on 1 October to almost 100% on 2 October indicating saturation and presumably cloud formation. However, the SH slightly decreases from about  $4 \text{ g kg}^{-1}$  on 1 October to about  $3.3 \text{ g kg}^{-1}$  on 2 October thus indicating less moist air on 2 October than on 1 October. The investigation of the synoptic situation at 500 hPa and of the tropopause fields (not shown here) indicated the existence of an upper trough over western Europe on 1 October, which moved eastwards over central Europe on 2 October thus affecting the alpine sites. Already on the 3 October a cut-off detached from the upper trough system and moved southwards over Italy while at the same time an upper ridge extending from the Azores high towards northeast started affecting western and Central Europe. The 4-days back-trajectories on 1 October indicate horizontal transport at the same level from the Atlantic Ocean while on 2 October there is a shift in transport with air masses advected to Zugspitze from about 900 hPa already one day before (presumably boundary layer air) with the source region located over Italy and west Mediterranean.

Although transport of boundary layer air with low  $^7\text{Be}$  concentration cannot be excluded as a partial explanation of the very low  $^7\text{Be}$  observed at Zugspitze, it is anticipated that wet scavenging is the most plausible explanation. This is suggested because the SH measurements indicate less moist air on 2 October than on 1 October while the RH measurements indicate saturation on 2 October.

*Case II (4 October 1996)—high  $^7\text{Be}$  concentration:* Fig. 6 shows clearly an abrupt increase of  $^7\text{Be}$  up to  $16 \text{ mBq m}^{-3}$  from 3 October to 4 October. At the same time, both SH and RH values decreased down to  $1 \text{ g kg}^{-1}$  and 20%, respectively, while the daily ozone concentration also increased up to 60 ppbv indicating transport of dry air masses rich in ozone. The synoptic situation at 500 hPa on 3 and 4 October (not shown here) is characterized by a high-pressure system extending northeastwards from the Azores high towards western and Central Europe. The tropopause was relatively high over the alpine region. Radiosonde measurements over Payerne reveal an increase of the tropopause height of about 4 km from 2 to 4 October. The 4-days back-trajectories on 3 October (12 and 18 UTC) at Zugspitze indicate downward transport from about 350 hPa over Greenland and North Atlantic 2 days ago, while the tropopause fields at this area on 1 October show tropopause heights dropping down to

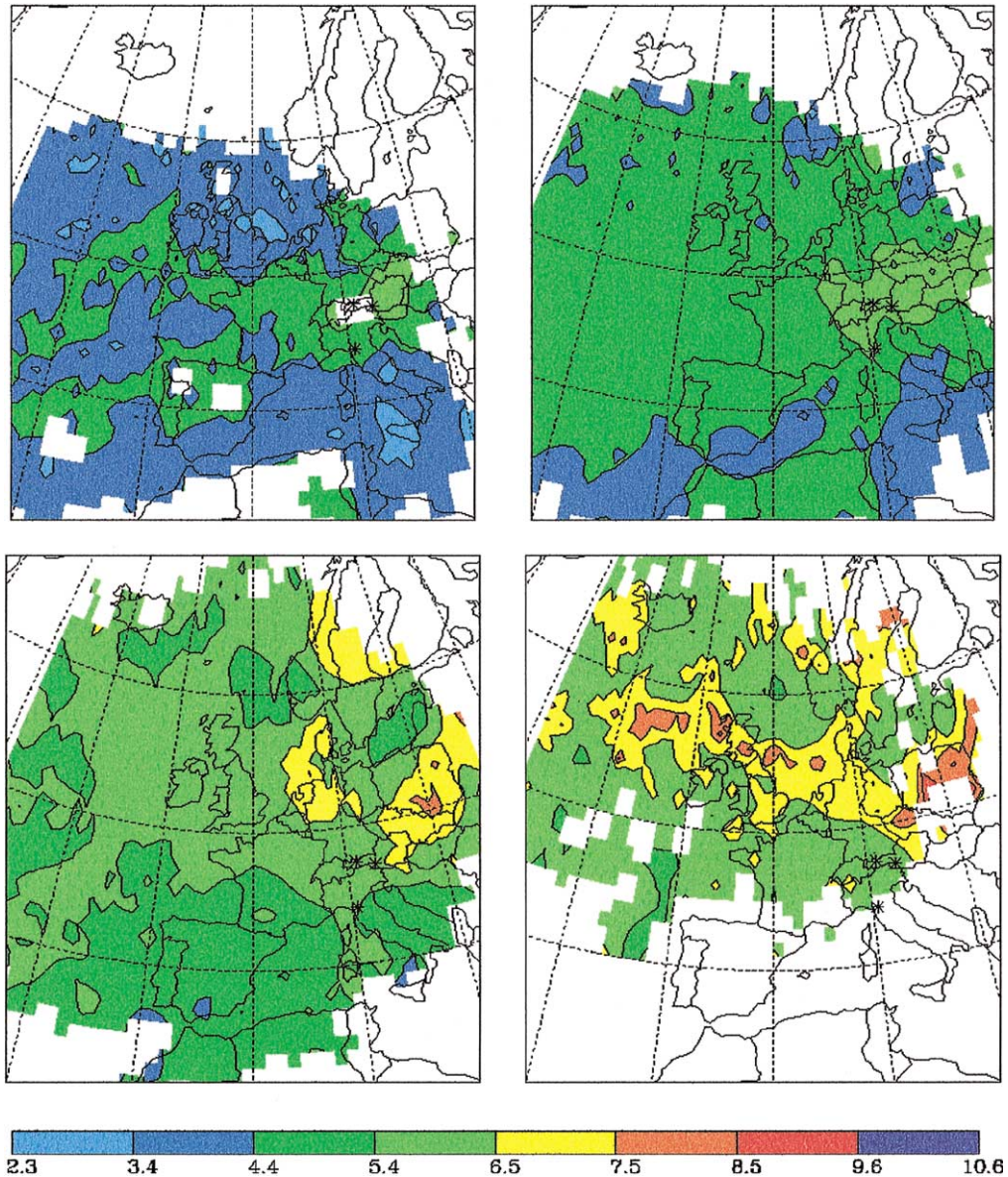


Fig. 5. Three-dimensional concentration fields of  $^7\text{Be}$  obtained with trajectory statistics for below 1500 m (upper left), 1500–3000 m (upper right), 3000–4500 m (lower left), and above 4500 m (lower right). Grid cells for which information from fewer than 20 measurements was available, were left blank. The locations of SBK, MTC and ZUG are marked with asterisks.

about 320 hPa. The 4-days back-trajectories on 4 October (00, 06, 12, and 18 UTC) show downward transport from about 500 hPa one to two days ago with the source area located at North Atlantic and Scandinavia. Similarly to Zugspitze, the other alpine stations showed also high  $^7\text{Be}$  concentrations on 4 October. Back-trajectories at Sonnblick on 4 October (00 UTC) indicated downward transport from about 340–350 hPa

2 days ago over North Atlantic and Scandinavia while the tropopause fields dropped down to 320 hPa over this area on 2 October. From this analysis it can be assumed that the abrupt increase of  $^7\text{Be}$  at Zugspitze and the other alpine stations on 4 October was related to downward transport from the lower stratosphere/upper troposphere of air rich in  $^7\text{Be}$  during a STE event over North Atlantic/Scandinavia. This was perhaps one of

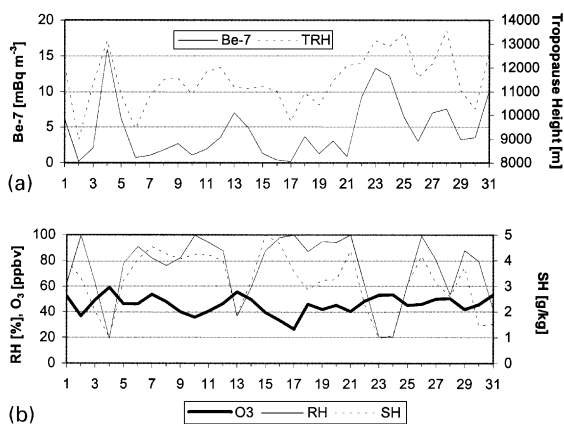


Fig. 6. Cases presentation during October 1996: (a)  ${}^7\text{Be}$  concentration (solid line) and tropopause height (dashed line), (b) surface ozone concentration (thick solid line), relative humidity (thin solid line) and specific humidity (dashed line).

the clearest cases of a stratospheric intrusion: see Stohl et al. (2000) for a description.

*Case III (22–24 October 1996)—high  ${}^7\text{Be}$  concentration:* The  ${}^7\text{Be}$  concentration at Zugspitze increases up to  $9 \text{ mBq m}^{-3}$  on 22 October, then reaches  $13 \text{ mBq m}^{-3}$  on 23 October and remains at high concentration levels ( $12 \text{ mBq m}^{-3}$ ) on 24 October (Fig. 6). Ozone also shows a slight increase during these days while both RH and SH values decrease down to about 20% and  $1 \text{ g kg}^{-1}$ , respectively. The tropopause over Payerne shows a gradual increase during these days. The synoptic patterns at 500 hPa indicate the gradual development of an upper ridge over central Europe. The same result is supported by the tropopause fields. The 4-days back trajectories on 23 and 24 October (00 UTC) reveal downward transport from a level of about 500 hPa 2 days ago, with the source region located at North Atlantic (north to England) and Scandinavia. However, the 4-days back-trajectories on 22 October (at 00 UTC) point towards a distant upper tropospheric source (lower stratospheric source cannot be excluded) over the North Atlantic ocean, close to the Canadian coast. It is hence anticipated that downward transport from middle to upper troposphere within the persistent anticyclonic system over central Europe from 22 to 24 October is a plausible explanation for the increase of  ${}^7\text{Be}$  concentration at Zugspitze during these days, although an indirect influence from STE cannot be discarded.

It should be also pointed out that the relatively high  ${}^7\text{Be}$  concentration at Zugspitze on 13 and 28 October (Fig. 6) associated with relatively high tropopause heights, was also found to be related with downward transport from the middle to upper troposphere in the presence of upper ridges.

### 3.6. Seasonal variation of the ${}^7\text{Be}$ concentrations

Because of the episodic nature of  ${}^7\text{Be}$  events, it is rather difficult to see a clear seasonal variation of the  ${}^7\text{Be}$  concentrations presented in Fig. 2, although the maximum values seem to be more frequent during the summer. However, the mean monthly  ${}^7\text{Be}$  values reveal a seasonality at all four stations (Fig. 7).

At all sites a distinct annual cycle exists with a late summer maximum in July–August. An interesting point is the secondary maximum observed in January–February especially at SBK and MTC. It is mainly due to the increased  ${}^7\text{Be}$  levels during February 1998 at all sites (for MTC there are no measurements during February 1996 and 1997), which can be attributed to the relatively higher tropopause during this month and also coincides with the secondary maximum in absolute frequency of stratospheric air intrusions found by Stohl et al. (2000) at ZUG and SBK. The minimum concentrations are generally met in winter, but the monthly means also reveal a minimum in April (ZUG, SBK, MTC), which is not in accordance with the expected spring maximum in STE suggested by Danielson and Mohnen (1977) and also Appenzeller et al. (1996). However, for the interpretation of the April minimum one should bear in mind that April 1998 was not a typical April, having an average tropopause height about 600 m lower than the previous years. Finally, one can notice that the lowest monthly concentration levels are found at ZUG, also inducing a minimum to the amplitude of the variation due to the seasonal cycle.

In order to derive information concerning the main mechanisms controlling the late-summer peak in the  ${}^7\text{Be}$  concentrations (see Fig. 7), supplementary correlation coefficients were calculated between the monthly means of  ${}^7\text{Be}$  and the meteorological and atmospheric parameters. The results indicate that the best and most consistent predictor of the seasonality of the  ${}^7\text{Be}$  concentrations for all stations is tropopause height, which is also object to a summer maximum seasonality, with calculated correlation coefficients of +0.76, +0.56, and +0.60 for JFJ, ZUG, and SBK, respectively (all coefficients significant at the 95% confidence level). Many other stations on both hemispheres show highest  ${}^7\text{Be}$  activity concentrations during the warm season and lowest concentrations during the cold season, which can be attributed to more efficient vertical mixing in the warm season due to enhanced solar heating and thus downward transport to the lower troposphere of  ${}^7\text{Be}$  produced in the upper troposphere or the stratosphere (Feely et al., 1989).

## 4. Summary and conclusions

Three years of  ${}^7\text{Be}$  data measured at four high-altitude stations at the Alps and Northern Apennines were used

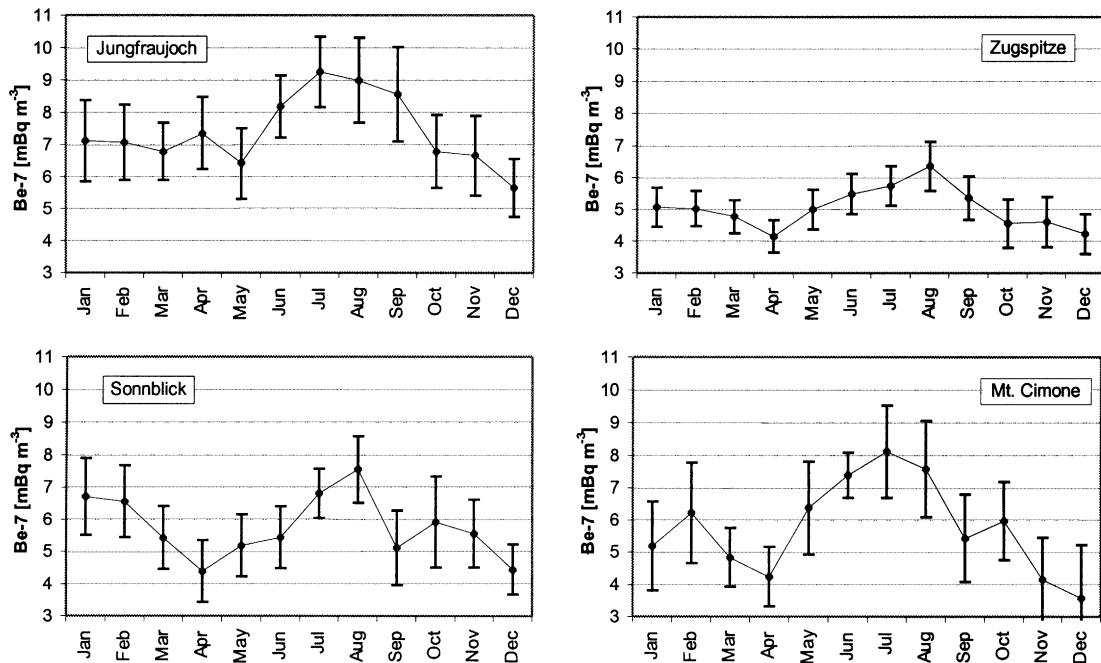


Fig. 7. Seasonal variation of the <sup>7</sup>Be concentrations derived from a three years data record. The error bars correspond to the 95% confidence level.

together with a set of meteorological and atmospheric parameters such as the tropopause height, relative and specific humidity and also in conjunction with 3D back trajectories, in order to investigate the climatology of <sup>7</sup>Be and study the mechanisms that govern <sup>7</sup>Be concentration levels.

A frequency distribution analysis, performed on each <sup>7</sup>Be record, revealed the existence of two concentration classes, one comprising the lower values with a mean about 1.5 mBq m<sup>-3</sup> and another one comprising the higher values with a mean around 6 mBq m<sup>-3</sup>. Further analysis on meteorological data such as tropopause height, relative and specific humidity, supported a transition class between the two modes of the distribution at 3–4 mBq m<sup>-3</sup> and postulated a second transition class of about 9–11 mBq m<sup>-3</sup>, above which <sup>7</sup>Be concentrations are expected to be strongly affected by STE processes. Comparison of the <sup>7</sup>Be concentrations between the stations gave significant correlations (+0.53 for JFJ versus ZUG, +0.42 for JFJ versus SBK and +0.7 for ZUG versus SBK), because they are all affected by the same larger-scale synoptic patterns.

Cross-correlation analysis was performed between <sup>7</sup>Be and meteorological and atmospheric parameters, using both original and deseasonalized data. The strongest correlation was found with relative humidity (negative correlation) depicting the importance of wet scavenging as a controlling mechanism for the day-to-day varia-

bility and with back-trajectories and tropopause height (positive correlation) showing that the upper level synoptic situation and downward transport are important controlling factors. Especially, the 3-days back-trajectories indicate a middle/upper tropospheric source of the highest <sup>7</sup>Be at all alpine stations while the positive correlation of the tropopause height with <sup>7</sup>Be implies downward transport within anticyclonic conditions. It should be noted that there is no clear indication from the back-trajectories height for the direct influence of stratospheric air on the high <sup>7</sup>Be concentrations at the three alpine sites but the indirect influence should not be underestimated as it is also implied from the source pathway of the high <sup>7</sup>Be concentrations. The positive correlation with surface ozone was difficult to decompose and interpret due to its complicated behavior concerning photochemical factors. For example, the fact that anticyclonic conditions favor at the same time downward mixing of higher <sup>7</sup>Be, intense photochemical ozone production and thermal convection of ozone precursors from the atmospheric boundary layer, poses great difficulties to attribute their correlation to a common upper troposphere/lower stratosphere source.

Trajectory statistics showed that low <sup>7</sup>Be concentrations typically originate from lower-altitude subtropical ocean areas, while high concentrations arrive from the north and high altitudes, as is characteristic for stratospheric intrusions. All the <sup>7</sup>Be controlling mechanisms

implied from the climatological study were also briefly investigated in three representative case studies during October 1996, which revealed the applicability of these mechanisms in reality.

Finally,  $^7\text{Be}$  concentrations were found to have a distinct annual cycle with a late-summer maximum, but this is apparent only in the monthly averages because  $^7\text{Be}$  concentrations are highly episodic. Correlation coefficients were also calculated on monthly means of the data, indicating that the main predictor of the seasonality of the  $^7\text{Be}$  concentrations is tropopause height, which reflects the stronger mixing of upper tropospheric with lower tropospheric air in summer.

### Acknowledgements

One of the authors, E. Gerasopoulos, is kindly supported by the Greek State Scholarship Foundation under Contract No. 2955 (32nd program, 1998–1999). This study was carried out within STACCATO (Contract No. EVK2-CT1999-00050), a project funded by the European Commission under the Fifth Framework Programme. Measurements were carried out during VOTALP, a project of the European Commission under the Fourth Framework Programme (Contract No. ENV4-CT1995-0025). We also thank the Swiss Meteorological Institute (SMI) at Payerne for providing the tropopause data. We wish to acknowledge EMPA Dübendorf for providing the filter samples at Jungfraujoch and also thank the Swiss Agency for the Environment, Forests and Landscape BUWAL for the meteorological and ozone data measured at Jungfraujoch by the National Air Pollution Monitoring Network (NABEL).

### References

- Appenzeller, C., Holton, J.R., Rosenlof, K.H., 1996. Seasonal variation of mass transport across the tropopause. *Journal of Geophysical Research* 101, 15071–15078.
- Austin, J.F., Follows, M.J., 1991. The ozone record at Payerne: an assessment of the cross-tropopause flux. *Atmospheric Environment* 25A (9), 1873–1880.
- Benioff, P.A., 1956. Cosmic-ray production rate and mean removal time of Beryllium-7 from the atmosphere. *Physical Review* 104, 1122–1131.
- Bithell, M., Vaughan, G., Gray, L.J., 2000. Persistence of stratospheric ozone layers in the troposphere. *Atmospheric Environment* 34, 2563–2570.
- Bonasoni, P., Evangelisti, F., Bonafe, U., Ravegnani, F., Calzolari, F., Stohl, A., Tositti, L., Tubertini, O., Colombo, T., 2000. Stratospheric ozone intrusion episodes recorded at Mt. Cimone during the VOTALP project: case studies. *Atmospheric Environment* 34, 1355–1365.
- Brost, R.A., Feichter, J., Heimann, M., 1991. Three-dimensional simulation of  $^7\text{Be}$  in a global climate model. *Journal of Geophysical Research* 96, 22423–22445.
- Danielsen, E.F., 1968. Stratospheric–tropospheric exchange based on radioactivity, ozone and potential vorticity. *Journal of the Atmospheric Sciences* 25, 502–518.
- Danielsen, E.F., Mohnen, V., 1977. Ozone transport, in situ measurements, and meteorological analysis of tropopause folding. *Journal of Geophysical Research* 82, 5867–5877.
- Dutkiewicz, V.A., Husain, L., 1985. Stratospheric and tropospheric components of  $^7\text{Be}$  in surface air. *Journal of Geophysical Research* 90, 5783–5788.
- ECMWF, 1995. User Guide to ECMWF Products 2.1, Meteorological Bulletin M3.2, ECMWF, Reading, UK.
- Elbern, H., Kowol, J., Sladkovic, R., Ebel, A., 1997. Deep stratospheric intrusions: a statistical assessment with model guided analysis. *Atmospheric Environment* 31, 3207–3226.
- Feely, H.W., Larsen, R.J., Sanderson, C.G., 1989. Factors that cause seasonal variations in Beryllium-7 concentrations in surface air. *Journal of Environmental Radioactivity* 9, 223–249.
- Gäggeler, H.W., 1995. Radioactivity in the atmosphere. *Radiochemica Acta* 70/71, 345–353.
- Gavini, M.B., Beck, J.N., Kuroda, P.K., 1974. Mean residence time of the long-lived radon daughters in the atmosphere. *Journal of Geophysical Research* 79, 4447–4452.
- Husain, L., Coffey, P.E., Meyers, R.E., Cederwall, R.T., 1977. Ozone transport from stratosphere to troposphere. *Geophysical Research Letters* 4, 363–365.
- Jaenicke, G., 1988. Atmospheric physics and chemistry in meteorology. In: Fischer, R. (Ed.), *Physical and Chemical Properties of Air*. *Laudelt-Boernstein Series, Group V, 4b*. Springer, Berlin, pp. 391–457.
- Kentarchos, A.S., Davies, T.D., Zerefos, C.S., 1998. A low latitude stratospheric intrusion associated with a cut-off low. *Geophysical Research Letters* 25, 67–70.
- Koch, D.M., Jacob, D.J., Graustein, W.C., 1996. Vertical transport of tropospheric aerosols as indicated by  $^7\text{Be}$  and  $^{210}\text{Pb}$  in a chemical tracer model. *Journal of Geophysical Research* 101, 18651–18666.
- Koch, D.M., Mann, M.E., 1996. Spatial and temporal variability of  $^7\text{Be}$  surface concentrations. *Tellus* 48B, 387–396.
- Lal, D., Malhotra, P.K., Peters, B., 1958. On the production of radioisotopes in the atmosphere by cosmic radiation and their application to meteorology. *Journal of Atmospheric and Terrestrial Physics* 12, 306–328.
- Lal, D., Peters, B., 1962. Cosmic ray produced isotopes and their applications to problems in geophysics. In: *Progress in Cosmic Ray and Elementary Particle Physics, Vol. 6*. North-Holland, New York, pp. 3–74.
- Lal, D., Peters, B., 1967. Cosmic ray produced radioactivity on the Earth. *Handbuch der Physik* 46, 551–612.
- Masarik, J., Beer, J., 1999. Simulation of particle fluxes and cosmogenic nuclide production in the Earth's atmosphere. *Journal of Geophysical Research* 104, 12099–12111.
- O'Brien, K., 1979. Secular variations in the production of cosmogenic isotopes in the Earth's atmosphere. *Journal of Geophysical Research* 84, 423–431.

- Papastefanou, C., Ioannidou, A., 1995. Aerodynamic size association of  $^7\text{Be}$  in ambient aerosols. *Journal of Environmental Radioactivity* 26, 273–283.
- Reiter, R., Munzert, K., Kanter, H.J., Potzl, K., 1983. Cosmogenic radionuclides and ozone at a mountain station at 3.0 km a.s.l. *Archiv für Meteorologie, Geophysik und Bioclimatologie, Serie B* 32, 131–160.
- Reiter, R., Kanter, H.-J., Jäger, H., Müller, H., Munzert, K., 1984. Balance of the tropospheric ozone and its relation to stratospheric intrusions indicated by cosmogenic radionuclides. Combined Annual Report Part XI and Part XII. US Department of Energy, Contract No. DE-AC02-76EV03425.
- Roelofs, G.J., Lelieveld, J., 1997. Model study of the influence of cross-tropopause  $\text{O}_3$  transports on tropospheric  $\text{O}_3$  levels. *Tellus* 49, 38–55.
- Seibert, P., Kromp-Kolb, H., Baltensberger, U., Jost, D.T., Schwikowski, M., 1994. Trajectory analysis of high-alpine air pollution data. In: Gryning, S.E., Milanm, M.M. (Eds.), *Air Pollution Modelling and its Application*, X. Plenum Press, New York, pp. 595–596.
- Scheel, H.E., Sladkovic, R., Kanter, H.J., 1999. Ozone variations at the Zugspitze (2962 m a.s.l.) during 1996–1997. In: Borrel, P.M., Borrel, P. (Eds.), *Proceedings of EUROTRAC-2 Symposium 98*. WIT Press, Southampton, pp. 260–263.
- Schuepbach, E., Davies, T.D., Massacand, A.C., 1999. An unusual springtime ozone episode at high elevation in the Swiss Alps: contributions both from cross-tropopause exchange and from the boundary layer. *Atmospheric Environment* 33, 1735–1744.
- Sladkovic, R., Munzert, K., 1990. *Lufthygienisch-klimatologische Überwachung im bayerischen Alpenraum*. IfU Report 908080, Abschlußbericht, Abschnitt VI/4.
- Stohl, A., Wotawa, G., Seibert, P., Kromp-Kolb, H., 1995. Interpolation errors in wind fields as a function of spatial and temporal resolution and their impact on different types of kinematic trajectories. *Journal of Applied Meteorology* 34, 2149–2165.
- Stohl, A., Seibert, P., 1998. Accuracy of trajectories as determined from the conservation of meteorological tracers. *Quarterly Journal of Royal Meteorological Society* 125, 1465–1484.
- Stohl, A., Spichtinger-Rakowsky, N., Bonasoni, P., Feldmann, H., Memmesheimer, M., Scheel, H.E., Trickl, T., Hubener, S., Ringer, W., Mandl, M., 2000. The influence of stratospheric intrusions on alpine ozone concentrations. *Atmospheric Environment* 34, 1323–1354.
- Tositti, L., Hübener, S., Kanter, H.J., Ringer, W., Tobler, L., Sandrini, S., 2001. Intercomparison of sampling and measurement of Be-7 in air at four high-altitude locations in Europe. *Atmospheric Environment*, submitted.
- UNSCEAR, 2000. Sources and effects of ionising radiation. United Nations Scientific Committee on the Effects of Atomic Radiation. United Nations, New York.
- Vaughan, G., Price, J.D., 1991. On the relation between total ozone and meteorology. *Quarterly Journal of Royal Meteorological Society* 117, 1281–1298.
- Zanis, P., Schuepbach, E., Gäggeler, H.W., Hübener, S., Tobler, L., 1999. Factors controlling Beryllium-7 at Jungfrauoch in Switzerland. *Tellus* 51B, 789–805.